doi.org/10.36721/PJPS.2026.39.6.176.1

Proteome-based identification and validation of NXPE3 in childhood acute lymphoblastic leukaemia

Najia Tabassum[1], Yamna Khurshid[2], Basir Syed[3], Aftab Ahmed[3], Sadia Muhammad[4], Rehan Imad[2] and Talat Mirza[2]*

[1]Department of Pathology, Ziauddin University, Karachi, Pakistan
[2]College of Molecular Medicine, Ziauddin University, Karachi, Pakistan
[3]Department of Biomedical and Pharmaceutical Sciences, School of Pharmacy, Chapman University, Irvine, CA 92618, United States
[4]Department of Pediatric Oncology, Indus Hospital and Health Network, Karachi, Pakistan

Abstract: **Background**: Childhood acute lymphoblastic leukaemia (cALL) tends to metastasize to central nervous system. Treatment with antileukemic agents against CNS leukaemia is an essential component for cure in ALL. Hence, it is essential to identify biomarkers for CNS infiltration. Proteomics, supported by mass spectrometry, is the platform for exploring biomarkers in various biological samples, contributing to translational research. **Objectives**: This study aimed to identify the plasma proteome profile of children across different risk groups of cALL. Neurexophilin and PC-esterase family, member 3 (NXPE3), was validated. The protein-protein interactions (PPI) of NXPE3 were evaluated with bioinformatics analyses. **Methods**: Plasma samples from 15 patients with B-ALL standard risk (SR), B-ALL high risk (HR) and T-ALL high risk (HR), were analysed using LC-MS/MS. NXPE3 protein was validated in all risk groups using ELISA. To compare the NXPE3 values across groups, the Kruskal-Wallis test was applied. A $p\text{-}value < 0.05$ was considered significant. STRING database was used for PPI. **Results**: LC MS/MS analysis showed upregulation of NXPE3 in B-ALL SR. Upon ELISA validation, a high plasma concentration of NXPE3 was observed in B-ALL SR, 4.37±1.84 ng/ml (95% CI 3.31, 5.44), consistent with LC MS/MS findings. A lower concentration of NXPE3 was observed in B-ALL HR 2.68±1.34 ng/ml and T-ALL HR 2.38±0.92ng/ml. The findings were statistically significant. The PPI of NXPE3 highlighted its involvement in multiple processes, including gene expression, cytoskeletal organisation and neuronal function. **Conclusion**: This is the first report of NXPE3 in cALL. NXPE3 was identified as a potential biomarker for assessing CNS infiltration in cALL. Further studies are recommended to explore its role in leukemogenesis.

Keywords: Acute lymphoblastic leukaemia; Mass spectrometry; Proteomics

Submitted on 08-11-2025 – Revised on 23-12-2025 – Accepted on 07-01-2026

INTRODUCTION

Acute lymphoblastic leukaemia (ALL) is the most common cancer in children and the leading cause of death from disease in this age group (Kakaje *et al*., 2020). It is characterised by abnormal proliferation of B- or T-lymphoblasts that infiltrate the bone marrow (BM), peripheral blood and extramedullary sites. According to the cell of origin, there are two subtypes of ALL: B-ALL and T-ALL. B-ALL is the most prevalent, accounting for 80-85% of cases and generally carries a favourable prognosis. T-ALL is less common and is associated with a poorer prognosis (Pastorczak *et al*., 2021). The incidence of childhood ALL (cALL) in Pakistan is 20.8% (Aslam *et al*., 2021).

The risk stratification of cALL into high-risk (HR) and standard-risk (SR) categories is based on specific prognostic factors. The initial risk stratification is based on the National Cancer Institute (NCI) criteria. i.e. SR includes patients ≤10 years and TLC count $\leq 50 \times 10^9$/L and HR constitute ≥10 years of age, or TLC $\geq 50 \times 10^9$/L. T-ALL falls under HR due to high chances of mortality and relapse (Hiroto Inaba, 2024). Additional risk factors considered are CNS status and cytogenetics (Meraj *et al*., 2020). cALL has a propensity to metastasise to the central nervous system (CNS) through upregulation of chemokine receptors and/or adhesion molecules (Gull *et al*., 2025). CNS involvement is detected in 3-5% of patients at initial diagnosis and in 30-40% of patients with relapse(Gull *et al*., 2025). It is a standard practice in the treatment of cALL for all patients to receive CNS -directed therapy, which typically includes intrathecal methotrexate (IT MTX) (Wu *et al*., 2022). Patients classified with CNS1 status (no blasts in CSF) typically receive fewer doses of IT MTX compared to those with initial CNS involvement, i.e. CNS2 (WBC ≤5 with blasts in CSF) and CNS3 (WBC ≥5 with blasts in CSF) (Heilmann *et al*., 2023). However, CNS-directed therapy causes neurocognitive impairments and secondary CNS malignancies. Hence, it is essential to explore new biomarkers and druggable targets in cALL to minimise the risk of overtreatment and neurotoxic effects (Enlund *et al*., 2024).

Proteomics is a technology that combines experimentation and data analysis to examine the composition, structure, expression and interactions between proteins at the cellular

**Corresponding author:* e-mail: deanresearch@zu.edu.pk

level (Cui *et al*., 2022). Mass spectrometers' technological advancements have enabled the protein-based molecular characterisation of cancers (Lu *et al*., 2025). Proteomics, enabled by MS and bioinformatics, provides comprehensive tools for exploring cancer biology, making it an attractive avenue for translating bench-to-bedside research. There is limited literature on the proteomics of cALL in various biological fluids. The proteins validated so far include plasma aggrecan core protein, alpha-2-HS-glycoprotein, coagulation factor XIII A chain, gelsolin, prefoldin 5-α, transthyretin, interferon-γ (IFN-γ), ADAM17, ATG3 and PFDN5-α in plasma, exosomes, bone marrow and CSF of patients with ALL (Broto *et al*., 2020, Calderon-Rodríguez *et al*., 2019, Xavier *et al*., 2022, Zhu *et al*., 2022). The identified proteins were associated with inflammation, signal transduction and chemotherapy-induced CNS damage, highlighting their involvement in leukemogenesis (Calderon-Rodríguez *et al*., 2019, Broto *et al*., 2020, Mo *et al*., 2019). However, the literature is limited, and each study identifies a different set of proteins, emphasising the need for further research. Most data are from developed countries, as mass spectrometry facilities require specialised expertise and advanced laboratory equipment.

Investigating the cALL proteome in Pakistani children is crucial given their unique exposures, risk factors and genetic background, which differ from those in high-income countries (Gull *et al*., 2025). In this study, the plasma proteome profile of different risk groups of cALL: B-ALL SR, B-ALL HR and T-ALL HR was explored using LC/MS-MS. Neurexophilin and PC-esterase family member 3 (NXPE3) was validated, as it localised to the brain. The protein-protein interactions of NXPE3 were evaluated with bioinformatics analyses. This is the first time NXPE3 has been reported in cALL.

MATERIALS AND METHODS

Study population

A total of sixty participants (15 per group: B-ALL SR, B-ALL HR, T-ALL HR, and controls) were included for LC-MS/MS analysis. ELISA validation was performed on 56 individual samples (14 per group) (Fig S1).

Clinical workup and risk stratification

This is a case-control study. Samples were collected from January 2019 to December 2022. All clinical workup was carried out at the clinical laboratory of the Indus Hospital, Karachi. Children 1-16 years diagnosed with ALL with a complete clinical workup were included in the study. Children with partially treated infantile leukaemia were excluded. A complete blood count (CBC) was performed using the haematological analyser Coulter DxH 900 (Beckman Coulter, USA). Leukocytosis was confirmed on review of the peripheral smear. Bone marrow aspiration was performed and lymphoblasts >20% confirmed the diagnosis of ALL. To identify the lineage, a four-colour FACS (fluorescent-activated cell sorting) Calibre flow cytometer (Becton Dickson, Bioscience) was used. The panel of monoclonal antibodies to B-cell-associated antigens used were CD79a, CD19, CD22 and CD10, T cell was CD3, CD1a, CD5, CD4, CD8. For cytogenetics, the 2016 WHO classification of lymphoid neoplasms was followed. The conventional Giemsa banding (G-banding) technique was used for numerical chromosomal abnormalities. Their results were interpreted in accordance with the International System for Cytogenetic Nomenclature (ISCN)(Mcgowan-Jordan *et al*., 2020). FISH (fluorescent in situ hybridisation) was carried out using Cytovision MB8, Leica Biosystems, on bone marrow aspirate to visualise structural chromosomal abnormalities. Probes by Metasystem Germany were tested for BCR: :ABL1, KM2TA, ETV6: :RUNX1 and Intrachromosomal amplification of chromosome 21(iAMP 21). Due to institutional policy, cytogenetic analysis of T-ALL was not performed. CSF analysis was performed to assess leukemic cell metastasis to the CNS. Slides were prepared, air-dried and stained with Wright's colourant. They were observed under a microscope to identify lymphoblasts. Findings were interpreted as: CNS1: no blasts in CSF; CNS2: WBC ≤5 with blasts in CSF, and CNS3: WBC ≥5 with blasts in CSF. On day 35, bone marrow aspiration was performed to assess morphological response to chemotherapy. The findings were categorised as follows: M1:≤ 5 blasts: in remission; M2: 5-25% blasts, M3: >25% blasts: non-remission. Based on the clinical findings in table 1, children were categorised into B-ALL SR. B-ALL HR and T-ALL HR.

Healthy controls

Children aged 1-16 years with a CBC profile within the normal range

Separation and storage of plasma of children with ALL and healthy controls

Approximately 5 mL of blood was collected into BD Vacutainer® EDTA tubes. Plasma was separated by centrifugation at 4°C and stored in multiple aliquots at -80°C in the multidisciplinary laboratory at Ziauddin University.

Pooling of samples

To ensure consistent dilution, an equal number of samples were included in each pool. Due to fewer T-ALL cases, each pool included 15 samples per group (B-ALL SR, B-ALL HR, T-ALL HR, and controls). After thawing, 200 µL of plasma from each sample was pooled into Falcon tubes. After collection, samples were thawed and pooled into four groups: B-ALL SR, B-ALL HR, T-ALL HR and controls. There were 15 samples in each group. 200 µl of plasma from each sample was collected and transferred to Falcon tubes.

Depletion of high-abundance proteins

Thermo Scientific™ Pierce™ Albumin Serum Depletion Kits, Catalog number 85160, were used. Depletion of the pooled samples was performed in triplicate following the manufacturer's protocol. The resin bottle was shaken to resuspend the resin. 400 µL of the slurry (corresponding to 200 µL of settled resin volume) was transferred into each spin column. The spin columns were placed in a 1.5–2.0 mL collection tube. They were centrifuged at 12,000 x g for 1 minute to remove excess liquid. The flow-through was discarded, and the spin columns were returned to the same collection tube.200 µL of binding/wash buffer was added to each spin column. The spin columns were centrifuged at 12,000 × g for 1 minute; the flow-through was discarded, and the columns were transferred to new collection tubes.50 µL of the albumin-containing sample was added to each column, incubated for 1–2 minutes and then centrifuged for 1 minute. The flow-through was reapplied to the spin column, incubated for 1–2 minutes, and then centrifuged. The flow-through was retained. The spin columns were then placed in a new collection tube. To release unbound proteins, the resin was washed by adding 50 µL of binding/wash buffer for each 20 µL of resin used. It was centrifuged, and the flow-through was retained.

In-solution digestion

Lysis buffer was made with 6M Guanidinium hydrochloride (GuHCl) in 100 mM Tris-HCl, pH 8.5, 5 mM tris (2-carboxyethyl) phosphine (TCEP), 10 mM chloro-acetamide (CAA). Samples were thawed and added to the lysis buffer at a 1:1 ratio. The solution was heated to 95 °C for 5 min. Sequence grade trypsin, working solution 1.0ug/µl was added and left overnight for digestion. All samples were dried on a SpeedVac. Samples were then shipped to the Chapman University School of Pharmacy in California, USA, for LC-MS/MS analysis.

Liquid chromatography and ultra-high-resolution mass spectrometry

Peptides digest was resuspended in 100ul solvent A. All samples were run in DDA mode first and then in DIA mode. Spectral libraries were created from the DDA data against human proteins from SwissProt database. The spectral libraries were then used to analyse the DIA data in Spectronaut. Chromatographic separation was done on a column Agilent, Advanced Bio, Peptide 2.7um, 2.1 x 250 mm using a Thermo Ultimate 3000-UHPLC system. A 65-minute curved gradient was used. Solvents were 0.1% formic acid in water (A) and 0.1% formic acid in acetonitrile (B). The column temperature was maintained at 35°C and the flow rate was set at 300 uL/min. The source ESI was set to the following parameters: an end-plate offset of 500 V, a nebuliser pressure of 2.0 Bar and a dry temperature of 200 °C. The capillary voltage is set at 4500 V, with a dry gas flow rate of 8.0 l/min. Funnel 1 and 2 RF are set to 400 and 600 Vpp, respectively. Ion energy to 5.0 eV and collision energy to 7.0 eV. The transfer time is 100.0 µs, pre-pulse storage to 10.0 µs and collision RF to 1500.0 Vpp, The DIA method optimised for the impact II mass spectrometer (Bruker), used 28 cycles to iterate through a 400-1000 m/z precursor window range while using a window size of 24 Da at a spectral acquisition rate of 14 Hz. This results in a total cycle time of 2 seconds. Each cycle started with one MS1 survey scan. Spectronaut Software (Version 19, Biognosys) was used for Data processing. The interference detection algorithm and cross-normalisation were applied to enhance quantification precision. The false discovery rate (FDR) was set at 0.01. Proteins identified with more than two matched peptides and a greater than 99% probability were accepted.

Identification of differentially expressed proteins

The dataset was processed in RStudio using the readxl package. Log2 fold change (Log2FC) and negative log10 of the *p*-value were calculated. Log2FC was calculated as the mean expression level in the risk group divided by that in the control group. Statistical significance was assessed by applying a negative log10 transformation to the *p*-value. Proteins with a log2FC>1 and a p-value <0.05 were considered upregulated, and those with a log2FC<1 and a *p*-value <0.05 were considered downregulated. Proteins that did not meet the criteria were considered non-significant.

Determination of plasma concentrations of NXPE3 by ELISA

Based on the MS findings, NXPE3 was selected for validation. Protein concentrations of NXPE3 were determined by enzyme-linked immunosorbent assay (ELISA) analysis in individuals of each group. The procedure was performed according to the manufacturer's instructions to measure NXPE3 (BT lab kit Cat No E7853Hu) levels and generate measurement standards. The absorbance of the standards and samples was determined by spectrophotometry at 450 nm using a microplate reader, Thermoscientific Multiskan Sky. Standard curves were created with protein concentration on the y-axis and average absorbance on the x-axis.

Bioinformatics analysis

Protein–protein interaction (PPI) network analysis of NXPE3 was performed using the online Search Tool for the Retrieval of Interacting Genes (STRING) database. Interactions with a combined score >0.4 were considered significant.

Statistical analysis

Data were analysed using GraphPad Prism10 software. For NXPE3 protein analysis, the data were first checked for normality, followed by the application of the Kruskal-Wallis test. $p \leq 0.05$ was considered significant. For clinical utility, a receiver operating characteristic (ROC) curve was generated.

Data deposition

The proteomic data have been deposited in ProteoSAFe in the public database. The ID/Ref numbers are MSV000100202 | PXD071925 (Syed, 2025).

RESULTS

NXPE3 was found to be upregulated in B-ALL SR

NXPE3 was found to be upregulated in B-ALL SR (Fig. 1). In B-ALL HR and T-ALL, no significant change was observed (not shown).

NXPE3 plasma concentration by ELISA

A high plasma concentration of NXPE3 was observed in B-ALL SR, at 4.37±1.84 ng/ml, compared with controls at 3.78±1.60 ng/ml. The findings were statistically insignificant. A lower concentration of NXPE3 was observed in B-ALL HR 2.68±1.34 ng/ml and T-ALL HR 2.38±0.92ng/ml compared to controls. By making multiple comparisons, a statistically significant difference was observed for B-ALL SR with B-ALL HR (p=0.01) and T-ALL HR (p=0.004) (Fig 2).

The area under the curve (AUC) of NXPE3 in B-ALL HR was 0.72 (0.540-0.919). The cutoff value was derived as 4.063 at 92.86% sensitivity and 50% specificity. The AUC of NXPE3 in T-ALL HR was 0.77 (0.059-0.944). The cutoff value was 4.24 at 100% sensitivity and 50% specificity (Figs. 3a and b). In B-ALL SR, AUC was 0.59(0.379, 0.814), which was unsatisfactory (not shown).

PPI network analysis of NXPE3

PPI analysis of NXPE3 comprised only large nodes, indicating that proteins with known 3D structures were included. The red-coloured node represented the NXPE3 protein (query protein) and the first shell of interactions with other proteins. The edges highlighted functional and protein-protein associations. Known interactions were extracted from curated databases and experimental analyses, whereas predicted interactions were based on gene neighbourhood, gene fusion and gene co-occurrence. Results also showed additional interactions based on text mining, co-expression and protein homology. Analysis revealed NXPE3 interactions with 10 proteins. Thicker / multi-colored edges, e.g., between ARL17A–LRRC37A2 or RRP38–ZNF611, indicate stronger interactions. Nodes clustered together, such as ARL17A–ARL17B–LRRC37A2, suggest functional relationships (Fig. 4).

DISCUSSION

The spread of leukemic blasts to the CNS constitutes a significant challenge to cALL treatment. In the quest to identify a novel biomarker for CNS infiltration, the proteomic profiles of different risk groups of cALL were explored. NXPE3 was found to be upregulated in B-ALL SR, whereas no significant finding was observed in B-ALL HR and T-ALL HR (Fig 1). Upon validation, NXPE3 concentration was higher in B-ALL SR, consistent with MS findings. In contrast, decreased concentrations were observed in both HR groups (Fig 2). There is limited literature available on NXPE3. NXPE3 is located on chromosome 3 (Song *et al*., 2023)The NXPE3 gene encodes a member of the neurexophilin family of neuropeptide-like glycoproteins. It is localised in the brain and interacts with alpha-neurexins, a presynaptic transmembrane receptor that facilitates adhesion between dendrites and axons (National Library of Medicine, 2025b, Zhang *et al*., 2025). Neurexins mediate diverse synaptic functions, including synapse assembly, presynaptic release machinery and postsynaptic receptor signalling (Khoja *et al*., 2023). The Human Protein Atlas reported NXPE3 detection in blood by MS (Atlas, 2025).

Researchers found NXPE3 upregulated in intracranial haemorrhage in mouse models. The use of dihydroergotamine decreased NXPE3 expression in neutrophils. They concluded that dihydroergotamine is a therapeutic target for NXPE3, potentially alleviating hypertension-related intracranial haemorrhage (Zhang *et al*., 2025). Their study findings clearly indicated that NXPE may be a potential marker for CNS disorders; however, further studies are needed to confirm this.

Human Protein Atlas reports NXPE3 as a prognostic marker for renal cancer (Sjöstedt *et al*., 2020, National Library of Medicine, 2025b). It is found to be downregulated in lung adenocarcinoma (Song *et al*., 2023). Since both malignancies metastasise to the CNS, it was hypothesised that NXPE3 may also serve as a potential biomarker of CNS metastasis. In the study, patients in the HR groups had CNS2 and CNS3 findings on CSF analysis. Additionally, initial high TLC count, T cell immunophenotype and certain cytogenetics such as MLL or BCR-ABL1 fusion are associated with a higher incidence of CNS leukaemia (Lenk *et al*., 2020). Hence, the lower NXPE3 concentration in B-ALL HR and T-ALL HR may be due to CNS infiltration. It is recommended that further studies on blood and CSF be conducted to confirm this.

Computational prediction of PPIs has become an essential tool for understanding the functions of unknown proteins, providing new insights into disease signal transduction pathways. As diseases and biological networks are closely interconnected, this approach helps in identifying therapeutic targets (Hamad *et al*., 2021). Bioinformatic analysis revealed PPIs for NXPE3 (Fig. 4).

Zinc finger protein 154 (ZNF154), Zinc finger protein 611 (ZNF611) and Zinc finger and BTB domain-containing protein 11 (ZBTB11) are involved in transcriptional regulation. Ribonuclease P protein subunit p38 (RPP38) is part of the multimeric ribonuclease P complex that enables ribonuclease P RNA binding activity. It is involved in tRNA 5'-leader removal, facilitating translation (National Library of Medicine, 2025c).

Table 1: Criteria for risk stratification

B-ALL SR	B-ALL HR	T-ALL HR
• All CNS1 • t(12;21) (ETV6/RUNX1) • Hyper diploidy: 51-65 chromosomes • In remission (MI post induction ≤5% blasts) • WBC ≤50,000 • Both genders	• CNS1,2 or 3 • WBC ≥50,000 • Both genders • t(9;22)(q34;qll): BCR-ABL1 or (t4;11) (q21;q23) MLL- AF4 • Hypodiploidy (<44 chromosomes) • In remission(MI post induction)	• Complete diagnostic workup • In remission

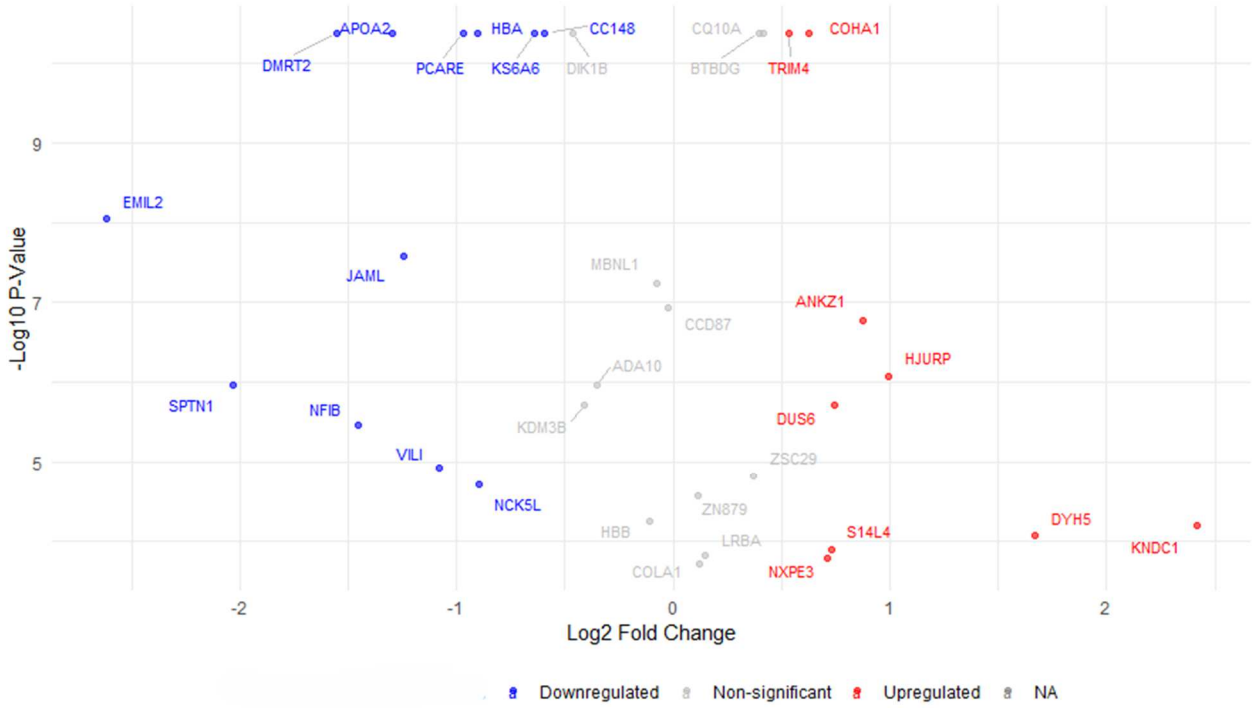

Fig. 1: Volcano plot showing up- and down-regulated proteins in B-ALL SR

NXPE3 was found to be upregulated in B-ALL SR (Fig. 1). In B-ALL HR and T-ALL, no significant change was observed (not shown).

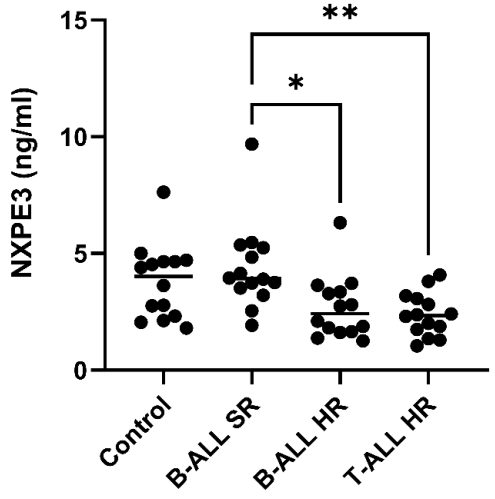

Fig. 2: Plasma levels of NXPE3 in B-ALL SR, B-ALL HR and T-ALL HR. Levels expressed as mean ±S.D, * indicates statistical significance,* $p < 0.05$ and** $p < 0.01$.

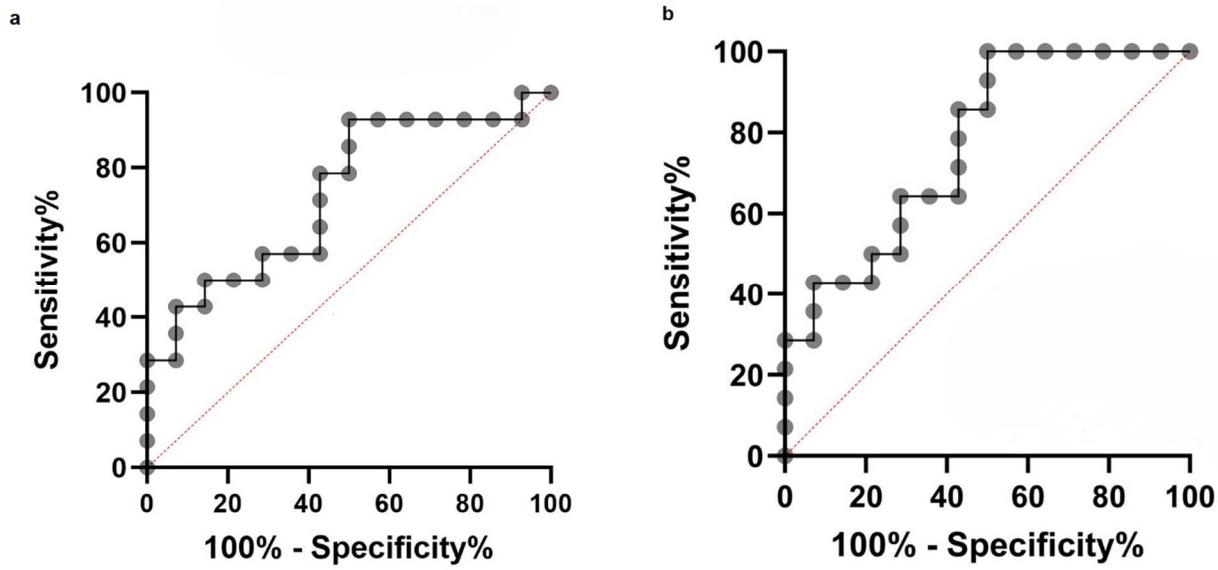

Fig. 3: ROC curve of a) B-ALL HR b) T-ALL HR

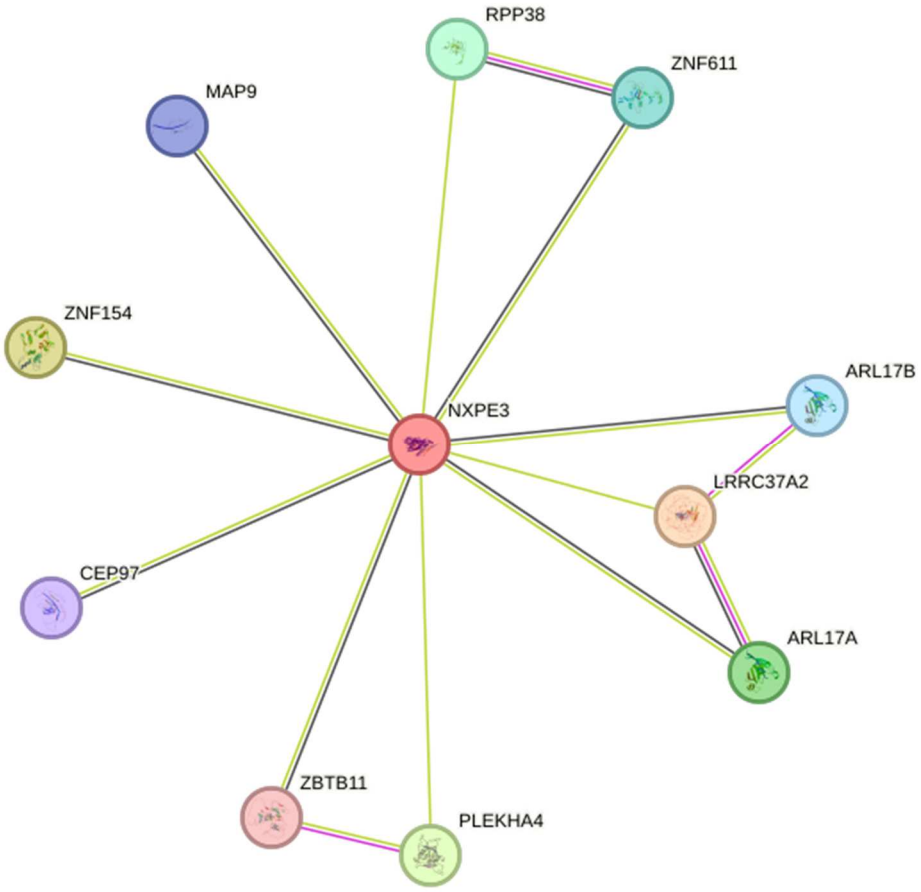

Fig. 4: Protein–protein interaction (PPI) of NXPE3

MAP9 is a microtubule-associated protein required for spindle function, mitotic progression and cytokinesis (National Library of Medicine, 2025a). ADP-ribosylation factor-like protein 17 (ARL17A) and ADP-ribosylation factor-like protein 17 (ARL17B) are GTP-binding proteins that function as an allosteric activator of the cholera toxin catalytic subunit, an ADP-ribosyltransferase. They are involved in protein trafficking (Uniprot, 2025) Leucine-rich repeat-containing protein 37A2 (LRRC37A) is a membrane-associated protein expressed in astrocytes. It

interacts with α-synuclein and co-localizes with Lewy bodies in Parkison disease (Bowles *et al*., 2022). ARL17A, ARL17B and LRR37A are located on chromosome 17 located at MAPT locus, which is associated with Parkinson's disease (Piacentini *et al*., 2025, Shani *et al*., 2023).The interactions of NXPE3's various proteins highlight its involvement in multiple processes, ranging from gene expression, cytoskeletal organisation, and neuronal function.

The study has a few limitations. Due to financial and technical limitations, as well as the unavailability of LC-MS/MS facility locally, pooling was necessary. Minimal residual disease data were unavailable; thus, only post-induction remission data were included.

CONCLUSION

NXPE3 was identified as a potential biomarker for assessing CNS infiltration in cALL. Bioinformatic analysis revealed the role of NXPE3 in various cellular and neuronal processes. Further studies are recommended to explore its role in leukemogenesis. This study makes a significant contribution to ongoing cALL research by identifying new biomarkers.

Acknowledgments
We would like to thank all the children and their parents or guardians for participating in this study. Additionally, we express our gratitude to the staff of the Pediatric Oncology ward at Indus Hospital for their dedication, and to Ms. Fariha Anum for her statistical expertise

Authors' contributions
N.T., Y.K. and T.M: Contributed to the study conception and design, as well as the drafting of the manuscript; S.M: Provided clinical samples and data; B.S. and A.A.: Performed the LC-MS/MS analyses. R.E. and N.T.: Conducted the ELISA experiments and performed all bioinformatics analyses; Y.K. and T.M.; Supervised the study. All authors contributed to the final editing and approved the manuscript for submission

Funding
This study was partially funded by Ziauddin University, but no funding number was assigned.

Data availability statement
The proteome of data generated and/or analysed during the current study is available at ProteoSAFe. ID/Ref numbers are MSV000100202 | PXD071925

Ethical approval
This study was done in collaboration with Ziauddin University and Indus Hospital, Karachi. This study was conducted in accordance with the Declaration of Helsinki. It was approved by the Institutional Review Board of Indus Hospital (IRD_IRB_2018_09_001) and Ziauddin University ERC (0430818NTPAT). All participants' parents or guardians signed informed consent before study enrollment. Assent was obtained from older children and written informed consent was obtained from their parents or guardians. This study was performed in adherence with the STROBE guidelines. See supplementary file for the STROBE checklist.

Conflict of interest
The authors declare no conflict of interest.

Supplementary data
https://www.pjps.pk/uploads/2026/04/SUP1775977068.pdf

REFERENCES

Aslam S, Shabana and Ahmed M (2021). Implications of ACMG guidelines to identify high-risk acute lymphoblastic leukemia patients with hereditary cancer susceptibility syndromes (HCSS) in a highly consanguineous population. *BMC pediatrics,* **21**(1): 282.

Atlas THP (2025). *NXPE3* [Online]. Available: https://www.proteinatlas.org/ENSG00000144815-NXPE3/blood [Accessed 19/12/25 2025].

Bowles KR, Pugh DA, Liu Y, Patel T, Renton AE, Bandres-Ciga S, Gan-Or Z, Heutink P, Siitonen A and Bertelsen S (2022). 17q21. 31 sub-haplotypes underlying H1-associated risk for Parkinson's disease are associated with LRRC37A/2 expression in astrocytes. *Mol. neurodegener.,* **17**(1): 48.

Broto GE, Correa S, Trigo FC, Santos ECD, Tomiotto-Pelissier F, Pavanelli WR, Silveira GF, Abdelhay E and Panis CJ (2020). Comparative analysis of systemic and tumor microenvironment proteomes from children with B-cell acute lymphocytic leukemia at diagnosis and after induction treatment. *Front Oncol,* **10**: 550213.

Calderon-Rodriguez SI, Sanabria-Salas MC and Umana-Perez AJ (2019). A comparative proteomic study of plasma in Colombian childhood acute lymphoblastic leukemia. *Plos one,* **14**: e0221509.

Cui M, Cheng C and Zhang L (2022). High-throughput proteomics: A methodological mini-review. *Lab Invest,* **102**(11): 1170-1181.

Enlund S, Sinha I, Neofytou C, Amor AR, Papadakis K, Nilsson A, Jiang Q, Hermanson O and Holm F (2024). The CNS microenvironment promotes leukemia cell survival by disrupting tumor suppression and cell cycle regulation in pediatric T-cell acute lymphoblastic leukemia. *Exp. Cell Res.,* **437**(2): 114015.

Gull S, Ahmad A, Iqbal L, Ain RU, Mushtaq W and Faizan M (2025). Treatment-related mortality in pediatric acute-lymphoblastic and myeloid leukemia: Experience from a low-and middle-income setting: Treatment-related mortality in pediatric acute-lymphoblastic and myeloid leukemia. *PJHS*, **6**(7): 114-119.

Hamad ON, Shamsir MS, Amran S and Abd-Alhasan AQ (2021). Protein network and functional analysis of human leukemia type's interaction. *Ann. Rom. Soc. Cell Biol.,* **25**(6): 9756-9770.

Heilmann J, Vieth S, Moricke A, Attarbaschi A, Barbaric D, Bodmer N, Colombini A, Dalla-Pozza L, Elitzur S and Izraeli S (2023). Effect of two additional doses of intrathecal methotrexate during induction therapy on serious infectious toxicity in pediatric patients with acute lymphoblastic leukemia. *Haematologica,* **108**(12): 3278.

Inaba H, Teachey D, Annesley C, Batra S, Beck J, Colace S and Stehman K (2025). Pediatric acute lymphoblastic leukemia, version 2.2025, NCCN clinical practice guidelines in oncology. *JNCCN*, **23**(2): 41-62.

Kakaje A, Alhalabi MM, Ghareeb A, Karam B, Mansour B, Zahra B and Hamdan O (2020). Rates and trends of childhood acute lymphoblastic leukaemia: An epidemiology study. *Sci. Rep.,* **10**(1): 1-12.

Khoja S, Haile MT and Chen LY (2023). Advances in neurexin studies and the emerging role of neurexin-2 in 16: autism spectrum disorder. *Front. Mol. Neurosci.,* 1125087.

Lenk L, Alsadeq A and Schewe DM (2020). Involvement of the central nervous system in acute lymphoblastic leukemia: opinions on molecular mechanisms and clinical implications based on recent data. *Cancer Metastasis Rev.,* **39**(1): 173-187.

Lu Y, Ma Y, Liu Q and Luo D (2025). Recent progress in mass spectrometry-based liquid biopsy for cancer detection and analysis: A comprehensive review. *TrAC Trends Anal. Chem*., **190**: 118291.

Mcgowan-Jordan J, Hastings RJ and Moore S (2020). *Iscn 2020: An International System for Human Cytogenomic Nomenclature (2020). Reprint of'Cytogenetic and Genome Research 2020, Vol.* **160***, No. 7-8'.* Karger Medical and Scientific Publishers, Switzerland, pp. 1-376.

Meraj F, Jabbar N, Nadeem K, Taimoor M and Mansoor N (2020). Minimal residual disease in childhood B Lymphoblastic leukemia and its correlation with other risk factors. *PJMS,* **36**(1): 20-26.

Mo F, Ma X, Liu X, Zhou R, Zhao Y and Zhou H (2019). Altered CSF proteomic profiling of paediatric acute lymphocytic leukemia patients with CNS infiltration. *Jour. Onco.,* **2019**(1): 3283629.

National Library of Medicine. (2025a). *MAP9 microtubule associated protein 9 [Homo sapiens (human)* [Online]. Available: https://www.ncbi.nlm.nih.gov/gene/79884 [Accessed 20/12/25].

National Library of Medicine. (2025b). *NXPE3 neurexophilin and PC-esterase domain family member 3 [Homo sapiens (human)]* [Online]. Available: https://www.ncbi.nlm.nih.gov/gene/91775 [Accessed 16th June 25].

National Library of Medicine. (2025c). *RPP38 ribonuclease P/MRP subunit p38 [Homo sapiens (human)]* [Online]. Available: https://www.ncbi.nlm.nih.gov/gene/10557 [Accessed 20/12/25 2025].

Pastorczak A, Domka K, Fidyt K, Poprzeczko M and Firczuk M (2021). Mechanisms of immune evasion in acute lymphoblastic leukemia. *Cancers,* **13**(7): 1536.

Piacentini K, Frohlich A, Pfaff A and Koks S (2025). Characterisation of the function of a lncRNA containing SINE-VNTR-Alu 67 to regulate the genes at the MAPT locus. *Exp. Bio. Med.,* **250**: 10805.

Shani S, Gana-Weisz M, Bar-Shira A, Thaler A, Gurevich T, Mirelman A, Giladi N, Alcalay RN, Goldstein O and Orr-Urtreger A (2023). MAPT Locus in Parkinson's disease patients of Ashkenazi origin: A stratified analysis. *Genes,* **15**(1): 46.

Sjostedt E, Zhong W, Fagerberg L, Karlsson M, Mitsios N, Adori C, Oksvold P, Edfors F, Limiszewska A and Hikmet F (2020). An atlas of the protein-coding genes in the human, pig, and mouse brain. *Science,* **367**(6482): eaay5947.

Song T, Yao M, Yang Y, Liu Z, Zhang L and Li W (2023). Integrative identification by Hi-C revealed distinct advanced structural variations in lung adenocarcinoma tissue. *Phenomics,* **3**(4): 390-407.

Syed A (2025). *Proteome-based identification and validation of NXPE3 in childhood acute lymphoblastic leukaemia* [Online]. Available: https://massive.ucsd.edu/ProteoSAFe/static/massive.jsp?redirect=auth [Accessed 16/02/26 2025].

Uniprot. (2025). *Q8IVW1 · ARL17_HUMAN* [Online]. Available: https://www.uniprot.org/uniprotkb/Q8IVW1/entry [Accessed 20/12/25 2025].

Wu SY, Short NJ, Nasr L, Dabaja BS and Fang PQ (2022). Central nervous system prophylaxis and treatment in acute leukemias. *Curr. Treat. Opt. Onco.,* **23**(12): 1829-1844.

Xavier T, Vijayachandran LS, Chandran R, Mony U, Augustine A, Sidharthan N, Ganapathy R, Keechilat P, Sundaram KR and Menon KNJ (2022). Interactome based identification and validation of prefoldin 5-α for prognosing CNS leukemia in B-ALL patients. *Sci. Rep.,* **12**: 15491.

Zhang M, Ning J, Liu J, Sun Y, Xiao N, Xu H and Chen J (2025). Peripheral blood immune landscape and NXPE3 as a novel biomarker for hypertensive intracerebral hemorrhage risk prediction and targeted therapy. *iMeta,* **4**(3): e70030.

Zhu S, Xing C, Li R, Cheng Z, Deng M, Luo Y, Li H, Zhang G, Sheng Y and Peng HJ (2022). Proteomic profiling of plasma exosomes from patients with B-cell acute lymphoblastic leukemia. *Sci. Rep.,* **12**(1): 11975.